Journal of Power Sources 242 (2013) 732–735

Contents lists available at SciVerse ScienceDirect

Journal of Power Sources

journal homepage: www.elsevier.com/locate/jpowsour

Short communication

Elastic moduli of polycrystalline $Li_{15}Si_4$ produced in lithium ion batteries

Zhidan Zeng [a,b,c], Nian Liu [d], Qiaoshi Zeng [b,c], Yang Ding [e], Shaoxing Qu [a], Yi Cui [c,f,**], Wendy L. Mao [b,c,*]

[a] Institute of Applied Mechanics, School of Aeronautics and Astronautics, Zhejiang University, Hangzhou 310027, PR China
[b] Geological and Environmental Sciences, Stanford University, Stanford, CA 94305, USA
[c] Photon Science and Stanford Institute for Materials and Energy Sciences, SLAC National Accelerator Laboratory, Menlo Park, CA 94025, USA
[d] Department of Chemistry, Stanford University, Stanford, CA 94305, USA
[e] Advanced Photon Source, Argonne National Laboratory, 9700 S. Cass Avenue, Argonne, IL 60439, USA
[f] Department of Materials Science and Engineering, Stanford University, Stanford, CA 94305, USA

HIGHLIGHTS

- Pure polycrystalline $Li_{15}Si_4$ was synthesized using a Li-ion battery.
- Crystalline $Li_{15}Si_4$ is stable under pressure up to 5.8 GPa.
- Elastic moduli for crystalline $Li_{15}Si_4$ was yielded.
- Bulk modulus for crystalline $Li_{15}Si_4$ follows Vegard's law.

ARTICLE INFO

Article history:
Received 26 February 2013
Received in revised form
13 May 2013
Accepted 23 May 2013
Available online 6 June 2013

Keywords:
Li-ion batteries
Silicon
Alloy
Elastic modulus
High pressure
In-situ X-ray diffraction

ABSTRACT

Pure body-center-cubic structured metastable polycrystalline $Li_{15}Si_4$ was synthesized in a Li-ion battery by electrochemically lithiating a thin Si wafer. Its stability and compressional behavior were investigated using *in-situ* high-pressure synchrotron X-ray diffraction (XRD) at room temperature. No phase transition was observed in polycrystalline $Li_{15}Si_4$ up to 5.8 GPa. A bulk modulus of 28.4(6) GPa was obtained for $Li_{15}Si_4$ by fitting the XRD data to a third order Birch–Murnaghan equation of state. We found that the bulk modulus of $Li_{15}Si_4$ follows a linear interpolation relationship between the bulk moduli for pure Li and Si. These results provide valuable experimental data to validate the theoretical calculation and are also important inputs for modeling the Li–Si system.

1. Introduction

Lithium ion batteries (LIB) represent important energy storage systems for portable electronics. However, the energy densities of current battery electrode materials are too low to meet the need of high energy density storage for electric vehicle applications. Therefore high capacity electrode materials are critical for next generation batteries. In terms of anode materials, silicon has the highest theoretical capacity (4200 mAh g^{-1}), ten times higher than currently used graphite (370 mAh g^{-1}), which together with its high Earth abundance and low discharge potential (*vs.* Li/Li^+) makes it a very promising anode candidate [1]. Despite the extraordinary future potential of silicon anodes, they face one major challenge which limits their practical application: enormous volume expansion (400%) and internal stress (average tensional or compressional stresses up to ~2 GPa) during cycling—which results in pulverization of the electrode and capacity fading [1–3].

* Corresponding author. Geological and Environmental Sciences, Stanford University, Stanford, CA 94305, USA. Tel.: +1 650 723 3718; fax: +1 650 725 2199.
** Corresponding author. Department of Materials Science and Engineering, Stanford University, Stanford, CA 94305, USA. Tel.: +1 650 723 4613; fax: +1 650 725 4034.
E-mail addresses: zhidanzeng@zju.edu.cn (Z. Zeng), yicui@stanford.edu (Y. Cui), wmao@stanford.edu (W.L. Mao).

0378-7753/$ – see front matter © 2013 Elsevier B.V. All rights reserved.
http://dx.doi.org/10.1016/j.jpowsour.2013.05.121

Significant effort has been devoted over the past decade to overcome this challenge. Many different forms of nanostructured silicon have been developed in order to help release the stress and minimize pulverization [4–7]. Knowledge of mechanical properties of Li–Si alloys is essential for further optimization of battery performance. Li–Si system has a well known phase diagram with many intermediate compounds, e.g. $Li_{12}Si_7$, Li_7Si_3, $Li_{13}Si_4$, $Li_{22}Si_5$. However, recent *in-situ* XRD and *in-situ* transmission electron microscope (TEM) studies have shown these stable Li–Si compositions are not formed during the electrochemical insertion of Li into Si. Instead, amorphous Li_xSi ($0 < x < 3.75$) is formed and a metastable crystalline $Li_{15}Si_4$ (c-$Li_{15}Si_4$) phase not present in the equilibrium Li–Si phase diagram appears upon full lithiation [8–10]. Therefore the mechanical properties, e.g. elastic moduli, of c-$Li_{15}Si_4$ and amorphous Li_xSi ($0 < x < 3.75$) are the key parameters determining the deformation and fracture of silicon anodes during battery cycling. These parameters are also critical inputs for modeling stress evolution, deformation and fracture of Si anodes. For instance, some simulations treat the elastic moduli of Li–Si alloys as a constant, while the modeling results (e.g. stress evolution in Si anode) are different when the elastic moduli change associated with Li insertion/extraction is taken into consideration [11,12]. However, due to experimental challenges, the stability under stress (especially at the level of a few GPa) and elastic moduli of c-$Li_{15}Si_4$ and amorphous Li_xSi are still unknown.

Theoretical calculations, i.e. static and molecular dynamics (MD) calculations based on density functional theory (DFT) have been used to predict the elastic moduli of Li–Si alloys [13–16], with significant disparity existing among simulation results for the bulk moduli of crystalline Li–Si alloys. Some calculations suggest the bulk modulus of Li–Si alloys decrease almost linearly with Li concentration, following the Vegard's law [17], while other studies predict Li–Si alloys should have higher bulk moduli than the values obtained by linear interpolation. [14–16] The bulk modulus of c-$Li_{15}Si_4$ derived from these studies varies from 30.2, 32.6, to 35.8 GPa [14–16]. Experimental data is still lacking, since the typical techniques for determining elastic moduli such as ultrasonic measurements is not applicable to c-$Li_{15}Si_4$, which is usually synthesized using electrochemical methods in very limited sample amounts, and is extremely chemically reactive in atmosphere. In this paper, we conducted *in-situ* high pressure X-ray diffraction (XRD) in a diamond anvil cell (DAC) on c-$Li_{15}Si_4$ derived from a Li-ion battery. The bulk modulus of c-$Li_{15}Si_4$ was determined from fitting the pressure–volume data to the equation of state (EOS) at room temperature, and the stability of c-$Li_{15}Si_4$ under pressure was investigated as well.

2. Experiment

2.1. Crystalline $Li_{15}Si_4$ synthesis

Li-ion batteries (two-electrode 2032-type coin cell) were prepared inside an Ar-filled glovebox using a Si wafer (50 μm thick) as the working electrode, Li metal as the counter and reference electrode, and a Celgard separator soaked in electrolyte. The mass of the Si wafer in a given experiment (ca. 0.7 mg) was measured using a microbalance (Sartorius SE2, 0.1 μg resolution). The electrolyte was 1.0 M $LiPF_6$ in 1:1 (w/w) ethylene carbonate/diethyl carbonate (EMD Chemicals). For electrochemical lithiation, linear sweep voltammetry was carried out using a Bio-logic VMP3 battery tester. The voltage was swept at 2 mV s^{-1} from the open circuit voltage to 5 mV *vs.* Li/Li^+, where it was held for ~40 h to ensure complete lithiation. The coin cell was then disassembled inside the glovebox and the Si wafer was completely converted to black c-$Li_{15}Si_4$ powders. The powders were washed with anhydrous diethyl carbonate and dried. The $Li_{15}Si_4$ was not exposed to air throughout the whole process.

2.2. High-pressure X-ray diffraction measurements

The c-$Li_{15}Si_4$ sample was loaded into a symmetric DAC in an Ar-filled glovebox. Two tiny ruby balls were loaded along with the sample as a pressure calibrant. Pressure was measured *in-situ* by monitoring the shift in the R1 fluorescence line of ruby [18]. The sample chamber was a 150 μm diameter hole drilled in a T301 stainless steel gasket, which is inert with respect to $Li_{15}Si_4$. After sample loading, the DAC was sealed (two diamond anvils press on each side of the stainless steel gasket tightly, making the sample chamber air-tight) before being removed from the glovebox. Helium was then loaded into the sample chamber as the pressure transmitting medium using the gas loading system at GSECARS, Advanced Photon Source (APS), Argonne National Laboratory (ANL) [19] . Helium is not only an inert gas, but also an excellent pressure transmitting medium for providing very hydrostatic conditions. *In-situ* high-pressure angle-dispersive XRD experiments were performed with a focused X-ray beam of 15 × 15 μm^2 (FWHM) at a wavelength of 0.3738 Å, at beamline 16 ID-B of the High Pressure Collaborative Access Team (HPCAT), APS, ANL. A MAR165 CCD was used for data collection, and the software package FIT2D was used to integrate the Debye–Scherrer rings [20].

3. Results and discussion

Crystalline $Li_{15}Si_4$ was reported to form in Li-ion batteries when the voltage is below 30 mV *vs.* Li/Li^+ [21]. In this study, the cutoff voltage of lithiation was set at 5 mV to ensure formation of c-$Li_{15}Si_4$. The specific capacity and current density profiles are shown in Fig. 1(a) and (b) as a function of time. The full capacity for lithiation

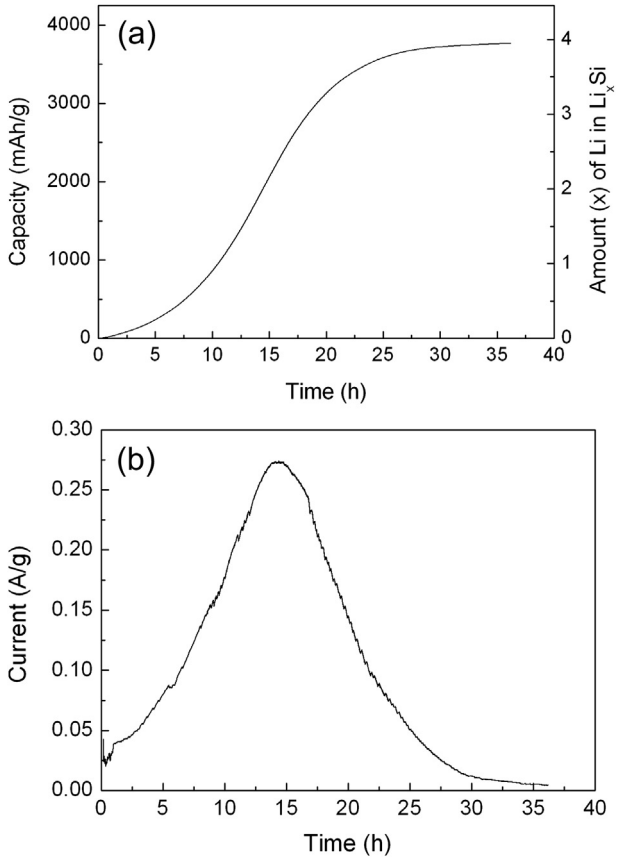

Fig. 1. Specific capacity (lefthand side *y*-axis) and the corresponding nominal Li amount (x) in Li_xSi (righthand side *y*-axis) (a), and current density (b) as a function of time for the Li-ion battery.

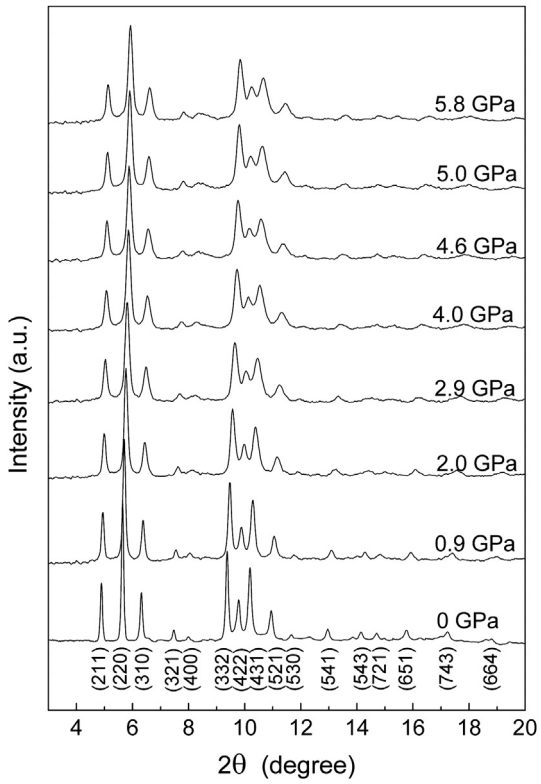

Fig. 2. *In-situ* XRD patterns for crystalline $Li_{15}Si_4$ under pressure at room temperature ($\lambda = 0.0738$ Å). The pattern at 0 GPa was taken before loading helium, with miller indices given at the bottom. All the high pressure patterns were taken after gas loading.

is 3766 mAh g^{-1}, corresponding to a nominal composition of $Li_{3.9}Si$. This calculated Li content is higher than that for $Li_{15}Si_4$ (or $Li_{3.75}Si$) due to solid-electrolyte-interphase (SEI) layer formation [22,23].

Fig. 2 shows the XRD patterns for c-$Li_{15}Si_4$ as a function of pressure up to 5.8 GPa. The structure of $Li_{15}Si_4$ at ambient pressure (0 GPa) was characterized in a sealed DAC prior to gas loading and is consistent with that from the literature, confirming that the as prepared sample is single phase polycrystalline $Li_{15}Si_4$ (space group: $I\bar{4}3d$) [24]. All the peaks are sharp and narrow, indicating the $Li_{15}Si_4$ was well crystallized. The results of refinement for the XRD patterns are shown in Table 1, in which the calculated d spacings (d_{cal}) agree with the observed values (d_{obs}) within 0.7‰. The obtained unit cell parameter (a) of c-$Li_{15}Si_4$ is 10.731(2) Å, which falls between the 10.685 Å reported by M. Obrovac et al. [21] and the 10.777 Å reported by T. Hatchard et al. [21,24]. Crystalline $Li_{15}Si_4$ is usually observed in *in-situ* studies of LIB, so it was thought to be a transient phase [8,9,21,24]. In our experiments, the c-$Li_{15}Si_4$ was taken out from the LIB and remained structurally unchanged when stored in an Ar-protected environment for 33 days at room temperature. This implies that "metastable" c-$Li_{15}Si_4$ is actually quite

Table 1
Unit-cell parameter (a) and d-spacings for c-$Li_{15}Si_4$ at different pressures.

|	d_{obs} (Å)	d_{cal} (Å)	d_{obs} (Å)	d_{cal} (Å)
P (GPa)	0		5.8	
211	4.3797	4.3810	4.1761	4.1790
220	3.7953	3.7941	3.6166	3.6191
310	3.3613	3.3613	3.2419	3.2371
332	2.2871	2.2879	2.1783	2.1824
422	2.1921	2.1905	2.0933	2.0895
431/510	2.1045	2.1046	2.0100	2.0075
521	1.9595	1.9592	1.8722	1.8689
a (Å)	10.731(2)		10.236(6)	

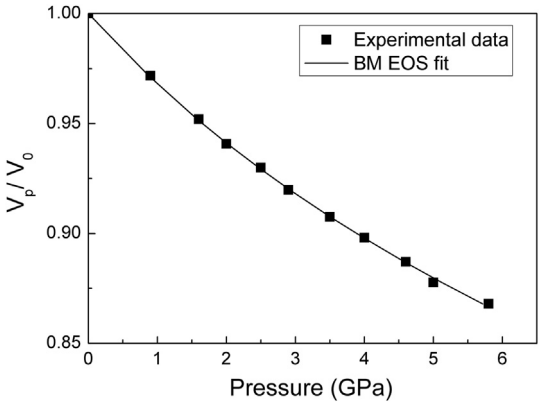

Fig. 3. Pressure versus fractional volume change for c-$Li_{15}Si_4$ up to 5.8 GPa. Symbols are experimental data, solid line is a third-order Birch–Murnaghan EOS fit to the measurements. Uncertainties in the volume determination are smaller than the size of the data points.

robust at room temperature, which is encouraging for future investigation of its physical and chemical properties.

As shown in Fig. 2, all the peaks shift systematically toward higher 2θ with the increase of pressure as a result of the lattice contraction under pressure. No new peaks were observed over the pressure range studied. The refinement results at 5.8 GPa (Table 1) indicate that the peaks can be well fit using the same $I\bar{4}3d$ space group, with differences between d_{cal} and d_{obs} of less than 1.9‰. This suggests that c-$Li_{15}Si_4$ maintains its original cubic symmetry even up to 5.8 GPa. Crystalline $Li_{15}Si_4$ has been reported to be sensitive to heating, decomposing into Li_7Si_3 and $Li_{13}Si_4$ at approximately 200 °C [25]. Our results suggest it is relatively stable under compressive stress. This may explain why c-$Li_{15}Si_4$ can be formed in Si anodes undergoing internal stresses up to 2 GPa.

The unit cell volume of c-$Li_{15}Si_4$ at different pressures can be calculated from the unit cell parameter (a), which was determined from refinement of the XRD patterns. Fig. 3 shows the unit cell volume change of c-$Li_{15}Si_4$ as a function of pressure. The unit cell volume decreases continuously and smoothly with increasing pressure, and the pressure–volume (P–V) data was fit to a third-order Birch–Murnaghan EOS (solid line in Fig. 3),

$$P = \frac{3B_0}{2}\left[\left(\frac{V_0}{V}\right)^{\frac{7}{3}} - \left(\frac{V_0}{V}\right)^{\frac{5}{3}}\right]\left\{1 + \frac{3}{4}(B_0' - 4)\left[\left(\frac{V_0}{V}\right)^{\frac{2}{3}} - 1\right]\right\}$$

where P is pressure, B_0 is the zero pressure bulk modulus, B_0' is the derivative of bulk modulus with respect to pressure, and V_0 and V are unit cell volumes at ambient and high pressure, respectively. This yielded for the first time, values for the bulk modulus and its pressure derivative of $B_0 = 28.4(6)$ GPa, and $B_0' = 4.9(4)$.

The bulk modulus is plotted together with results from calculations in Fig. 4. Our experimental data is consistent with the result from DFT calculations [14] with a difference around 5%, and is lower than the values predicted by the other two calculations [15,16]. According to Vegard's law which suggests the properties of an alloy can be estimated by a weighted averaging the properties of its constituent elements [17], a linear interpolation of the two experimental bulk moduli for pure Si and Li is plotted in Fig. 4. The bulk modulus of c-$Li_{15}Si_4$ we obtained in this work falls right on this line. In other words, it is consistent with Vegard's law. For the other Li–Si alloys, the experimental data for their bulk moduli is not available. Although there are some discrepancies among the results from different calculations, all the data points also generally follow the line. This implies the bulk moduli of crystalline Li–Si alloys can be estimated using Vegard's law. In addition, nanoindention experiments suggest

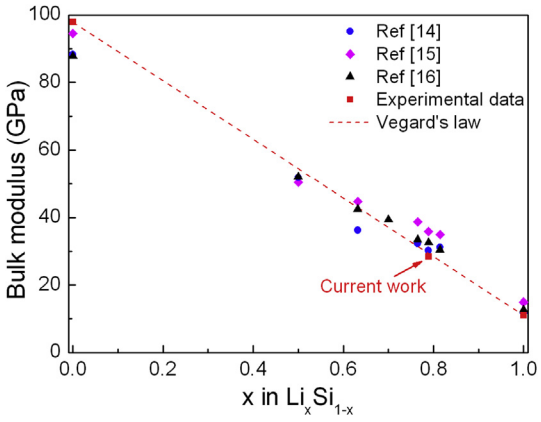

Fig. 4. Bulk moduli of crystalline Li_xSi_{1-x} alloys as a function of Li fraction derived from both simulations and experiments. Experimental data (square) for pure Si and Li are from Refs. [29] and Ref. [30] respectively. Error for the bulk modulus of c-$Li_{15}Si_4$ is smaller than the size of the data point. The other symbols represent data from theoretical calculations by V. Shenoy et al. (circle) [14], V. Chevrier et al. (diamond) [15] and H. Kim et al. (triangle) [16]. Dashed line connecting bulk modulus of Si and Li represents Vegard's law.

Young's modulus (E) of $Li_{15}Si_4$ is 12 GPa [26]. The Poisson's ratio (ν) and shear modulus (G) can then be derived from B and E using the following relations, as the c-$Li_{15}Si_4$ herein is polycrystal which can be approximated to be isotropic:

$$E = 3B\,(1 - 2\nu)$$

$$E = 2G\,(1 + \nu).$$

The shear modulus and Poisson's ratio are estimated to be G = 10 GPa and ν = 0.43. Note that some uncertainty may be introduced by the Young's modulus used in the calculation, as the Young's modulus herein is for a $Li_{15}Si_4$ thin film rather than its bulk counterpart.

As mentioned above, the bulk modulus of c-$Li_{15}Si_4$ can be estimated using Vegard's law. Vegard's law is usually valid in alloys composed of elements with similar atomic size and electronegativity [27]. Due to the significant difference in electronegativity for Li and Si (Pauling electronegativity is 0.98 for Li, 1.90 for Si), there is charge transfer between Li and Si atoms, and the covalent Si–Si bonds are replaced with ionic Li–Si bonds with increasing Li concentration [14,28]. In addition, Si (space group $Fd\bar{3}m$), Li (space group $Im\bar{3}m$) and their compounds (e.g. $Li_{15}Si_4$, space group $I\bar{4}3d$) have different crystal structures. Thus it is interesting that we can use Vegard's law to estimate the bulk moduli for this system. Although the underlying physics is still not clear, it does indicate that the mechanical behavior for compounds in the Li–Si system appears to be less sensitive to electronegativity and crystal structure.

4. Conclusion

In this work, pure polycrystalline $Li_{15}Si_4$ obtained from Li-ion batteries was investigated using *in-situ* high pressure X-ray diffraction. Metastable polycrystalline $Li_{15}Si_4$ persists up to 5.8 GPa without any phase transition. This may be one of the reasons why metastable c-$Li_{15}Si_4$ can be formed in LIB upon full lithiation with the associated huge internal stresses. The bulk modulus of $Li_{15}Si_4$ was determined from fitting XRD data to a third order Birch–Murnaghan EOS (B = 28.4(6) GPa). This is the first time that the bulk modulus of polycrystalline $Li_{15}Si_4$ has been obtained experimentally. It was found that the bulk moduli for both c-$Li_{15}Si_4$ and other crystalline Li–Si alloys follow a linear interpolation relationship between pure Li and Si moduli, i.e. Vegard's law. The shear modulus and Poisson's ratio of polycrystalline $Li_{15}Si_4$ were calculated given the bulk and Young's moduli. These results provide valuable experimental data to validate theoretical calculations and are also critical input for modeling the Li–Si system.

Acknowledgment

We thank Dr. Jiyong Zhao for help with our experiments. This work was supported as part of the EFree, an Energy Frontier Research Center funded by the US Department of Energy, Office of Science, Office of Basic Energy Sciences under Award No. DE-SG0001057. The experiments were performed at HPCAT (Sector 16), APS, ANL. HPCAT operations are supported by CIW, CDAC, UNLV and LLNL through funding from DOE-NNSA and DOE-BES, with partial instrumentation funding by NSF. APS is supported by DOE-BES, under Contract No.DE-AC02-06CH11357. Use of the gas loading system at GSECARS was supported by NSF (EAR-0622171, EAR 06-49658 and EAR 10-43050), DOE (DE-FG02-94ER14466) and COMPRES. Y.C. acknowledges the support from the Assistant Secretary for Energy Efficiency and Renewable Energy, Office of Vehicle Technologies of the U.S. Department of Energy under Contract No. DE-AC02-05CH11231, Subcontract No. 6951379 under the Batteries for Advanced Transportation Technologies (BATT) Program. Zhejiang University participants are supported by Zhejiang Provincial Natural Science Foundation of China (No. R6100325), the Science and Technology Innovative Research Team of Zhejiang Province (2009R50010) and the China Postdoctoral Science Foundation.

References

[1] B.A. Boukamp, G.C. Lesh, R.A. Huggins, J. Electrochem. Soc. 128 (1981) 725–729.
[2] M.J. Chon, V.A. Sethuraman, A. McCormick, V. Srinivasan, P.R. Guduru, Phys. Rev. Lett. 107 (2011) 045503.
[3] V.A. Sethuraman, M.J. Chon, M. Shimshak, V. Srinivasan, P.R. Guduru, J. Power Sources 195 (2010) 5062–5066.
[4] C.K. Chan, H.L. Peng, G. Liu, K. McIlwrath, X.F. Zhang, R.A. Huggins, Y. Cui, Nat. Nanotechnol. 3 (2008) 31–35.
[5] Y. Yao, M.T. McDowell, I. Ryu, H. Wu, N.A. Liu, L.B. Hu, W.D. Nix, Y. Cui, Nano Lett. 11 (2011) 2949–2954.
[6] T. Song, J.L. Xia, J.H. Lee, D.H. Lee, M.S. Kwon, J.M. Choi, J. Wu, S.K. Doo, H. Chang, W. Il Park, D.S. Zang, H. Kim, Y.G. Huang, K.C. Hwang, J.A. Rogers, U. Paik, Nano Lett. 10 (2011) 1710–1716.
[7] H. Wu, G. Chan, J.W. Choi, I. Ryu, Y. Yao, M.T. McDowell, S.W. Lee, A. Jackson, Y. Yang, L. Hu, Y. Cui, Nat. Nanotechnol. 7 (2012) 310–315.
[8] X.H. Liu, L.Q. Zhang, L. Zhong, Y. Liu, H. Zheng, J.W. Wang, J.H. Cho, S.A. Dayeh, S.T. Picraux, J.P. Sullivan, S.X. Mao, Z.Z. Ye, J.Y. Huang, Nano Lett. 11 (2011) 2251–2258.
[9] S. Misra, N. Liu, J. Nelson, S.S. Hong, Y. Cui, M.F. Toney, ACS Nano (2012) 5465–5473.
[10] J. Li, J.R. Dahn, J. Electrochem. Soc. 154 (2007) A156–A161.
[11] K.J. Zhao, W.L. Wang, J. Gregoire, M. Pharr, Z.G. Suo, J.J. Vlassak, E. Kaxiras, Nano Lett. 11 (2011) 2962–2967.
[12] R. Deshpande, Y. Qi, Y.T. Cheng, J. Electrochem. Soc. 157 (2010) A967–A971.
[13] Z. Cui, F. Gao, Z. Cui, J. Qu, J. Power Sources 207 (2012) 150–159.
[14] V.B. Shenoy, P. Johari, Y. Qi, J. Power Sources 195 (2010) 6825–6830.
[15] V.L. Chevrier, J.W. Zwanziger, J.R. Dahn, Can. J. Phys. 87 (2009) 625–632.
[16] H. Kim, C.Y. Chou, J.G. Ekerdt, G.S. Hwang, J. Phys. Chem. C 115 (2011) 2514–2521.
[17] A.R. Denton, N.W. Ashcroft, Phys. Rev. A 43 (1991) 3161–3164.
[18] H.K. Mao, P.M. Bell, J.W. Shaner, D.J. Steinberg, J. Appl. Phys. 49 (1978) 3276–3283.
[19] M. Rivers, V.B. Prakapenka, A. Kubo, C. Pullins, C.M. Holl, S.D. Jacobsen, High Pressure Res. 28 (2008) 273–292.
[20] A.P. Hammersley, S.O. Svensson, M. Hanfland, A.N. Fitch, D. Hausermann, High Pressure Res. 14 (1996) 235–248.
[21] M.N. Obrovac, L. Christensen, Electrochem. Solid State Lett. 7 (2004) A93–A96.
[22] Y.C. Yen, S.C. Chao, H.C. Wu, N.L. Wu, J. Electrochem. Soc. 156 (2009) A95–A102.
[23] S.P.V. Nadimpalli, V.A. Sethuraman, S. Dalavi, B. Lucht, M.J. Chon, V.B. Shenoy, P.R. Guduru, J. Power Sources 215 (2012) 145–151.
[24] T.D. Hatchard, J.R. Dahn, J. Electrochem. Soc. 151 (2004) A838–A842.
[25] Y. Wang, J. Dahn, J. Electrochem. Soc. 153 (2006) A2314–A2318.
[26] B. Hertzberg, J. Benson, G. Yushin, Electrochem. Commun. 13 (2011) 818–821.
[27] W.W. Porterfield, Inorganic Chemistry, a Unified Approach, Addison Wesley Publishing Co., 1984.
[28] V.L. Chevrier, J.W. Zwanziger, J.R. Dahn, J. Alloys Compd. 496 (2010) 25–36.
[29] H. Robert, in: Properties of Crystalline Silicon, INSPEC, The Institution of Electrical Engineers, London, 1999.
[30] D.R. Lide, in: 79th edition, CRC Press, Florida, 1998.